molecules

MDPI

Article

Design, Synthesis and Docking Studies of Flavokawain B Type Chalcones and Their Cytotoxic Effects on MCF-7 and MDA-MB-231 Cell Lines

Addila Abu Bakar [1], Muhammad Nadeem Akhtar [1,*], Norlaily Mohd Ali [2], Swee Keong Yeap [3], Ching Kheng Quah [4], Wan-Sin Loh [4], Noorjahan Banu Alitheen [5,*], Seema Zareen [1], Zaheer Ul-Haq [6] 🆔 and Syed Adnan Ali Shah [7] 🆔

[1]   Faculty of Industrial Sciences & Technology, University Malaysia Pahang, Lebuhraya Tun Razak, Kuantan 26300, Malaysia; addilaabubakar@gmail.com (A.A.B.); seema@ump.edu.my (S.Z.)
[2]   Faculty of Medicine and Health Sciences, University Tunku Abdul Rahman, Sungai Long 43400, Malaysia; norlailyma@gmail.com
[3]   Chine-ASEAN College of Marine Sciences, Xiamen University Malaysia, Jalan Sunsuria, Bandar Sunsuria, Sepang 43900, Malaysia; skyeap2005@gmail.com
[4]   X-ray Crystallography Unit, School of Physics, University Sains Malaysia, Penang 11800, Malaysia; ck.quah@hotmail.com (C.K.Q.); wansin_loh@live.com (W.-S.L.)
[5]   Department of Cell and Molecular Biology, Faculty of Biotechnology and Biomolecular Science, University Putra Malaysia, Serdang, Selangor Darul Ehsan 43400, Malaysia
[6]   Dr. Panjwani Center for Molecular Medicine and Drug Research, International Center for Chemical and Biological Sciences, University of Karachi, Karachi 75270, Pakistan; zaheer.qasmi@iccs.edu
[7]   Research Institute of Natural Products for Drug Discovery, Faculty of Pharmacy, University Teknologi MARA, Puncak Alam Campus, Bandar Puncak Alam 42300, Malaysia; benzene301@yahoo.com
*   Correspondence: nadeemupm@gmail.com (M.N.A.); noorjahan@upm.edu.my (N.B.A.); Tel.: +60-9-549-2393 (M.N.A.); Fax: +60-9-549-2766 (M.N.A.)

Abstract: Flavokawain B (**1**) is a natural chalcone extracted from the roots of *Piper methysticum,* and has been proven to be a potential cytotoxic compound. Using the partial structure of flavokawain B (FKB), about 23 analogs have been synthesized. Among them, compounds **8**, **13** and **23** were found in new FKB derivatives. All compounds were evaluated for their cytotoxic properties against two breast cancer cell lines, MCF-7 and MDA-MB-231, thus establishing the structure–activity relationship. The FKB derivatives **16** (IC_{50} = 6.50 ± 0.40 and 4.12 ± 0.20 µg/mL), **15** (IC_{50} = 5.50 ± 0.35 and 6.50 ± 1.40 µg/mL) and **13** (IC_{50} = 7.12 ± 0.80 and 4.04 ± 0.30 µg/mL) exhibited potential cytotoxic effects on the MCF-7 and MDA-MB-231 cell lines. However, the methoxy group substituted in position three and four in compound **2** (IC_{50} = 8.90 ± 0.60 and 6.80 ± 0.35 µg/mL) and **22** (IC_{50} = 8.80 ± 0.35 and 14.16 ± 1.10 µg/mL) exhibited good cytotoxicity. The lead compound FKB (**1**) showed potential cytotoxicity (IC_{50} = 7.70 ± 0.30 and 5.90 ± 0.30 µg/mL) against two proposed breast cancer cell lines. It is evident that the FKB skeleton is unique for anticancer agents, additionally, the presence of halogens (Cl and F) in position 2 and 3 also improved the cytotoxicity in FKB series. These findings could help to improve the future drug discovery process to treat breast cancer. A molecular dynamics study of active compounds revealed stable interactions within the active site of Janus kinase. The structures of all compounds were determined by ^{1}H-NMR, EI-MS, IR and UV and X-ray crystallographic spectroscopy techniques.

Keywords: chalcone synthesis; breast cancer cell lines; SARs; anti-cancer; flavokawain B derivatives

1. Introduction

Breast cancer (BC) is a complex disease, composed of several subtype receptors both at the molecular and clinical level. BC is still the leading causes of death globally in women [1–3]. Chalcones are α,β-unsaturated carbonyl compounds with two aromatic rings (ring A and B), conjugated double bonds and a completely delocalized π-electron system [4,5]. Chalcones and their related analogues display several pharmacological properties, such as anticancer [6–10], anti-inflammatory [11–14], antimalarial [15,16], antileishmanial [17,18], antimicrobial [19], antifungal [20], antioxidant [21–23] and anticonvulsant activities [24]. Chalcone derivatives show acetylcholinesterase, tyrosinase [25,26], and monoamine oxidase (MAO) [27] enzyme inhibitory activities. Chalcones have gained the strong attention from scientists searching for new pharmacological active analogs.

Flavokawain B (FKB) (**1**), is a main bioactive chalcone isolated from the roots of *Piper methysticum* [28], which exhibited strong cytotoxicity against various cancer cell lines [29–31]. In this study, we synthesized **1–23** FKB analogs by manipulating ring B with the various substituted benzaldehydes. The main purpose when designing this proposal was to observe the effects of ring B in the breast cancer cell lines and to establish the structure–activity relationship, to eventually help future drug discovery. Previously, we investigated the antinociceptive, cytotoxic and anti-inflammatory activities of FKB (**1**) in vitro and in vivo [32–36].

2. Results and Discussion

2.1. Chemistry

Flavokawain B derivatives (**1–23**) were synthesized by Claisen–Schmidt condensation reaction using the template of FKB (**1**) (Scheme 1). FKB comprises ring A (2′-hydroxy-4′,6′-dimethoxyacetophenone) and B (benzaldehyde). Among FKB derivatives, three chalcones (*E*)-3-(2,5-dimethoxyphenyl)-1-(2′-hydroxy-4′,6′-dimethoxyphenyl)prop-2-en-1-one (**8**), (*E*)-3-(2-fluorophenyl)-1-(2′-hydroxy-4′,6′-dimethoxyphenyl)prop-2-en-1-one (**13**) and (*E*)-3-(2-bromo-3-hydroxy-4-methoxyphenyl)-1-(2′-hydroxy-4′,6′-dimethoxyphenyl)prop-2-en-1-one (**23**) were found to be new FKB analogs (Figure 1). Previously, compound **13** was synthesized by Bandgar and used as an intermediate for the preparation of nitrogen-containing chalcones, however, the data were not published [37]. The structure of FKB derivatives (**1–23**) were characterized by detailed spectroscopic techniques. The presence of characteristic signals appeared in ^{1}H-NMR at δ 7.66–7.84 (*J* = 15–16 Hz) and 7.86–8.0 (*J* = 15–16 Hz) were assigned to α and β protons, respectively. The presence of carbonyl groups was supported by the signals at δ 191–193.45 in ^{13}C-NMR and 1625–1634 cm^{-1} in the IR spectrum, respectively. The complete assignments and spectral data of compounds **8**, **13** and **23** are given in Table 1, while the structure of compounds **7** and **9** was confirmed by the single X-ray crystallographic technique (Figure 2).
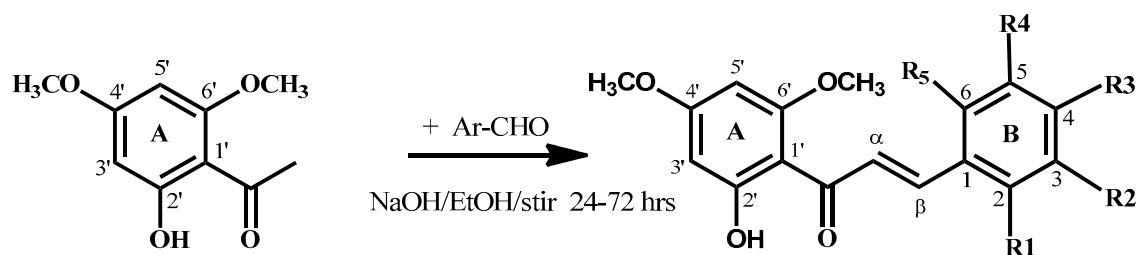
Scheme 1. Synthesis of flavokawain B derivatives **1–23**.

Table 1. ^{1}H- (600 MHz) and ^{13}C- (150 MHz) NMR data for compound **8**, **13** and **23**.

Carbon	8			13′			23		
	^{1}H (δ)	Multiplicity	^{13}C (δ)	^{1}H (δ)	Multiplicity	^{13}C (δ)	^{1}H (δ)	Multiplicity	^{13}C (δ)
1′	-	-	106.89	-	-	106.38	-	-	106.25
2′	-	-	162.36	-	-	162.57	-	-	161.84
3′	6.16	(d, J = 2.22 Hz, 1H)	94.38	6.11	(d, J = 2.40 Hz, 1H)	93.81	6.00	(d, J = 2.50 Hz, 1H)	93.86
4′	-	-	165.98	-	-	168.42	-	-	165.57
5′	6.13	(d, J = 2.46 Hz, 1H)	91.59	5.96	(d, J = 2.34 Hz, 1H)	91.29	5.88	(d, J = 2.35 Hz, 1H)	91.06
6′	-	-	165.98	-	-	166.37	-	-	165.55
1	-	-	124.18	-	-	124.40	-	-	127.05
2	-	-	153.65	-	-	134.87	-	-	113.28
3	7.06	(d, J = 9.06 Hz, 1H)	113.65	7.11	(m, 1H)	116.29	-	-	140.87
4	7.03	(d, J = 9.06 Hz, 1H)	113.58	7.18	(td, J = 7.56 Hz, 7.50 Hz, 1H)	131.28	-	-	149.86
5	-	-	153.16	7.59	(td, J = 7.56 Hz, 7.68 Hz, 1H)	129.73	6.78	(d, J = 8.55 Hz, 1H)	110.95
6	7.22	(brs, J = 2.76 Hz, 1H)	118.10	7.35	(m, 1H)	130.27	7.20	(d, J = 8.60 Hz, 1H)	118.85
α	7.84	(d, J = 15.80 Hz, 1H, H-α)	128.59	7.86	(d, J = 15.78 Hz, 1H, H-α)	123.73	7.67	(d, J = 15.45 Hz, 1H, H-α)	127.05
β	7.86	(d, J = 15.80 Hz, 1H, H-β)	137.83	8.00	(d, J = 15.78 Hz, 1H, H-β)	160.83	8.02	(d, J = 15.45 Hz, 1H, H-β)	144.09
OCH$_3$ (C4′)	3.84	(s, 3H)	56.62	3.84	(s, 3H)	55.78	3.75	(s, 3H)	56.15
OCH$_3$ (C6′)	3.89	(s, 3H)	56.58	3.91	(s, 3H)	55.60	3.85	(s, 3H)	55.63
OCH$_3$ (C2)	3.82	(s, 3H)	55.95	-	-	-	-	-	-
OCH$_3$ (C4)	-	-	-	-	-	-	3.81	(s, 3H)	56.22
OCH$_3$ (C5)	3.77	(s, 3H)	56.16	-	-	-	-	-	-
OH (C2′)	13.46	(s, 1H)	-	14.25	(s, 1H)	-	-	(s, 1H)	-
C=O	-	-	193.03	-	-	192.62	-	-	191.86
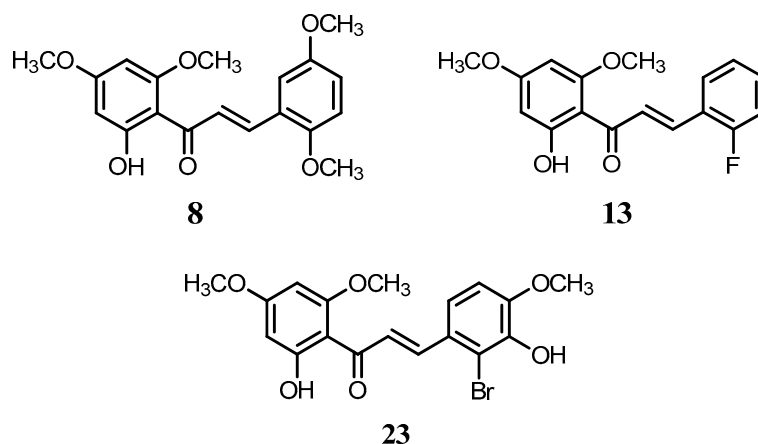
Figure 1. The structure of compounds **8**, **13** and **23**.
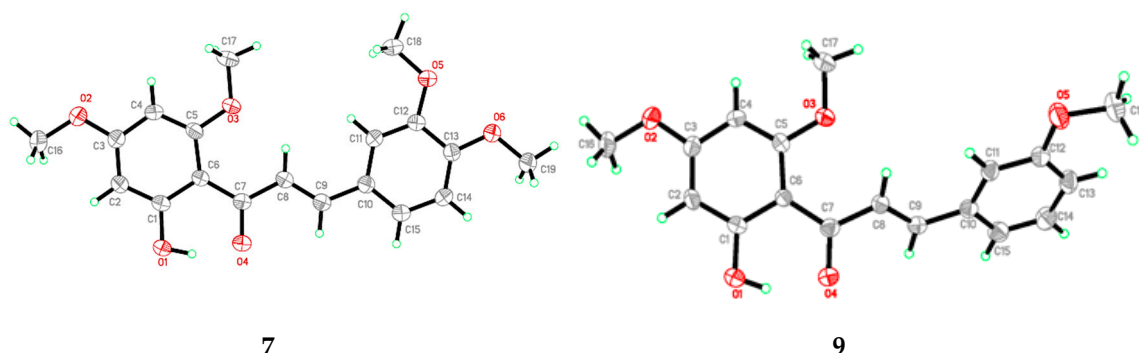

Figure 2. ORTEP diagram of compound **7** and **9**.

2.2. Structure–Activity Relationships

FKB derivatives **1**–**23** were screened against two breast cancer cell lines MCF-7 (human estrogen receptor positive breast cancer cells) and MDA-MB-231 (human estrogen receptor negative) breast cancer cell lines. FKB (**1**) still possessed greater cytotoxicity (IC_{50} = 7.70 ± 0.30 and 5.90 ± 0.30 µg/mL) compared to the majority of FKB derivatives. Of the 23 tested compounds, thirteen FKB derivatives recorded higher IC_{50} values than FKB (**1**). On the other hand, FKB derivatives **2**–**4**, **7**, **9**, **13**, **15**, **16** and **22** were recorded as having potential cytotoxic effects on both MCF-7 and MDA-MB-231 cells, compared to FKB (**1**), see Table 2. Among the FKB derivatives, compounds **13**, **15** and **16** showed slightly better cytotoxicity than FKB (**1**) and flavokawain A (FKA) (**2**) for MCF-7 cells.

Among the FKB derivatives with an IC_{50} value lower than 30 µg/mL, only compound **3** and **22** showed higher sensitivity to MCF-7 cells than MDA-MB-231, indicating that the modification of the FKB skeleton helps the selectivity between these two cell lines. In short, the FKB derivatives FKB-2F (**13**), FKB-3Cl (**15**) and FKB-2Cl (**16**) exhibited greater sensitivity to both tested cell lines, warranting further evaluation of their antitumor effects. It is well established that the anticancer properties of chalcones are due to the presence of α,β-unsaturated ketone moieties. Among the tested chalcones, the 2′ hydroxyl group in ring A is essential for the cytotoxicity, as has been studied against several biological assays, predominantly its anticancer properties [38,39]. The presence of electron-withdrawing and electron-donating groups effects the α,β-unsaturated system [38,40], which eventually effects the cytotoxicity. Generally, the electron-donating group in ring A improves the cytotoxic properties, as it affects the acidity of the 2′ hydroxyl group in ring A, while the electron-donating group in ring B, as in compound **5**, **6**, **8** and **10**, did not improve the IC_{50} values at 30 µg/mL (Table 2), which possibly due to the effects of the electron-donating group on the α, β-unsaturated system. Since the α,β-unsaturated system becomes more nucleophile and the Michael

receptor or protein cannot bind effectively thus activity decreases [38]. However, compounds **4** and **7** showed slightly better activity due to the selective position of the methoxy groups at **3**, **4** and **2**, **3**, which contributed less to the α,β-unsaturated ketone. In contrast, compounds with electron-withdrawing groups in ring B possessing 2Cl (**16**), 3Cl (**15**) and 2F (**13**) exhibited better cytotoxicity, see Table 2. The presence of the electron-withdrawing group in ring B, especially at position 2 and 3, as in **13** (2F), **15** (3Cl) and **16** (2Cl), contributed more to the enhancement of cytotoxicity against breast cancer cell lines (38, 39). While the presence of electron-withdrawing groups in compounds **13**, **15** and **16** pulling the electrons from the α,β-unsaturated ketone make it more electrophilic, so the receptor (nucleophile) possibly creates a strong interaction with the compound. While the electrons with the donating group, such as methoxy groups—especially at position 3, 4 or 3, 5 and 2, 4, 6, as in compounds **5**, **6**, **8**, **10**, **11**, cause rich in nucleophilicity and resonate the α,β-unsaturated carbonyl [41], eventually, the structure become less effective and binding or the interaction with the Michael receptor (nucleophile), and the compounds reduce the cytotoxic effects [38,39].

**Table 2.** IC$_{50}$ values (μg/mL) of FKB derivatives after 72 h treatment.

	Compounds Substituted Groups					IC$_{50}$ Values (μg/mL)	
Compounds	R1	R2	R3	R4	R5	MCF-7	MDA-MB-231
1	H	H	H	H	H	7.70 ± 0.30	5.90 ± 0.30
2	H	H	CH$_3$O	H	H	8.90 ± 0.60	6.80 ± 0.45
3	H	H	SCH$_3$	H	H	12.30 ± 1.40	18.10 ± 1.10
4	CH$_3$O	CH$_3$O	H	H	H	25.00 ± 1.80	21.10 ± 1.20
5	CH$_3$O	H	CH$_3$O	H	H	>30	>30
6	CH$_3$O	H	CH$_3$O	H	CH$_3$O	>30	>30
7	H	CH$_3$O	CH$_3$O	H	H	9.70 ± 0.70	8.30 ± 0.56
8	CH$_3$O	H	H	CH$_3$O	H	>30	>30
9	H	CH$_3$O	H	H	H	8.43 ± 0.40	7.22 ± 0.70
10	H	CH$_3$O	H	CH$_3$O	H	>30	>30
11	H	H	CH$_3$	H	H	>30	>30
12	CH$_3$O	H	H	H	H	>30	9.50 ± 0.60
13	F	H	H	H	H	7.12 ± 0.80	4.04 ± 0.30
14	H	H	F	H	H	>30	>30
15	H	Cl	H	H	H	5.50 ± 0.35	5.50 ± 0.40
16	Cl	H	H	H	H	6.50 ± 0.40	4.12 ± 0.20
17	H	H	Cl	H	H	>30	>30
18	H	H	Br	H	H	>30	>30
19	H	CH$_3$O	OH	H	H	>30	27.00 ± 1.50
20	H	NO$_2$	H	H	H	13.30 ± 3.10	17.10 ± 2.15
21	H	H	N(CH$_3$)$_2$	H	H	>30	20.5 ± 1.60
22	OH	H	H	Br	H	6.50 ± 0.35	14.16 ± 1.10
23	Br	OH	OCH$_3$	H	H	>30	>30

2.3. Computational Studies

The potential FKB derivatives **1**, **13**, **15** and **16** were subjected to rigid receptor docking, and the resulting poses were analyzed visually. The crystal structure of JAK2 in complex with a potent quinoxaline inhibitor, PDB: 3KRR, was downloaded in MOE and subjected to protein preparation. The results of a PASS prediction highlight the probability of the activity of these compounds as a caspase-3 stimulant, JAK2 expression inhibitor, and apoptosis agonist, as shown in Table S1. Caspase-3 belongs to the cystine–aspartic-acid protease family of proteins [42], known to play a fundamental role in the execution phase of cell death in apoptosis [43]. The activators of caspase-3, such as MX-2060 [12,44], Smac [45] and Leachianone A [46], induce apoptosis in various types of cancers.

The high Pa values of the compounds (0.892–0.924) allowed us to conclude that our newly-synthesized chalcone derivatives may exhibit anticancer effects by activating the caspase-3-dependent apoptotic pathway. Moreover, the cell-specific response of the chalcone derivatives can be explained partly by the fact that the human MCF-7 breast carcinoma cells completely lack caspase-3 expression as a result of a frameshift mutation [43,47]. This loss-of-function mutation has contributed to chemotherapeutic resistance in breast cancer [12,44]. The Janus kinase-2 (JAK2) protein is targeted by many anti-cancer drugs to produce their response [45,48]. As presented in

Table S1, our compounds may inhibit JAK2, with Pa values ranging from 0.821 to 0.878. We carried out a molecular docking simulation to establish the binding mode of the potent FKB derivatives with IC$_{50}$ values in single digits, namely **1**, **13**, **15** and **16**, with JAK2 (PDB:3KRR). All the compounds fit the active site of JAK2 wells, depicted in Figure 3. The docking results revealed that all the compounds mediated hydrophobic contacts with Val863 and Leu983. The methoxy group of the compounds interacted via an acceptor–donor hydrogen bonding motif to the Leu932 backbone. A hydrogen bond with Leu932 provided these compounds with anchorage in the cavity. In the case of compound **13** and **15**, an additional hydrogen bond was observed with Leu855 and Asp944, respectively. Analysis of the average duty cycle revealed that the most stable hydrogen bond pair was Arg938 and O2, and Leu932 and O3 in the **13** and **16** complexes, respectively. The binding profile of **13**-JAK2 shows equally high expression of three different host–guest pairs, Gly856, Leu855 and Lys857. Accurate characterization of protein–ligand interactions is indispensable for the drug design. Molecular dynamic simulation is a state-of-art technique that is used to characterize the time-dependent behavior for protein–ligand complex (See Supplementary Material).
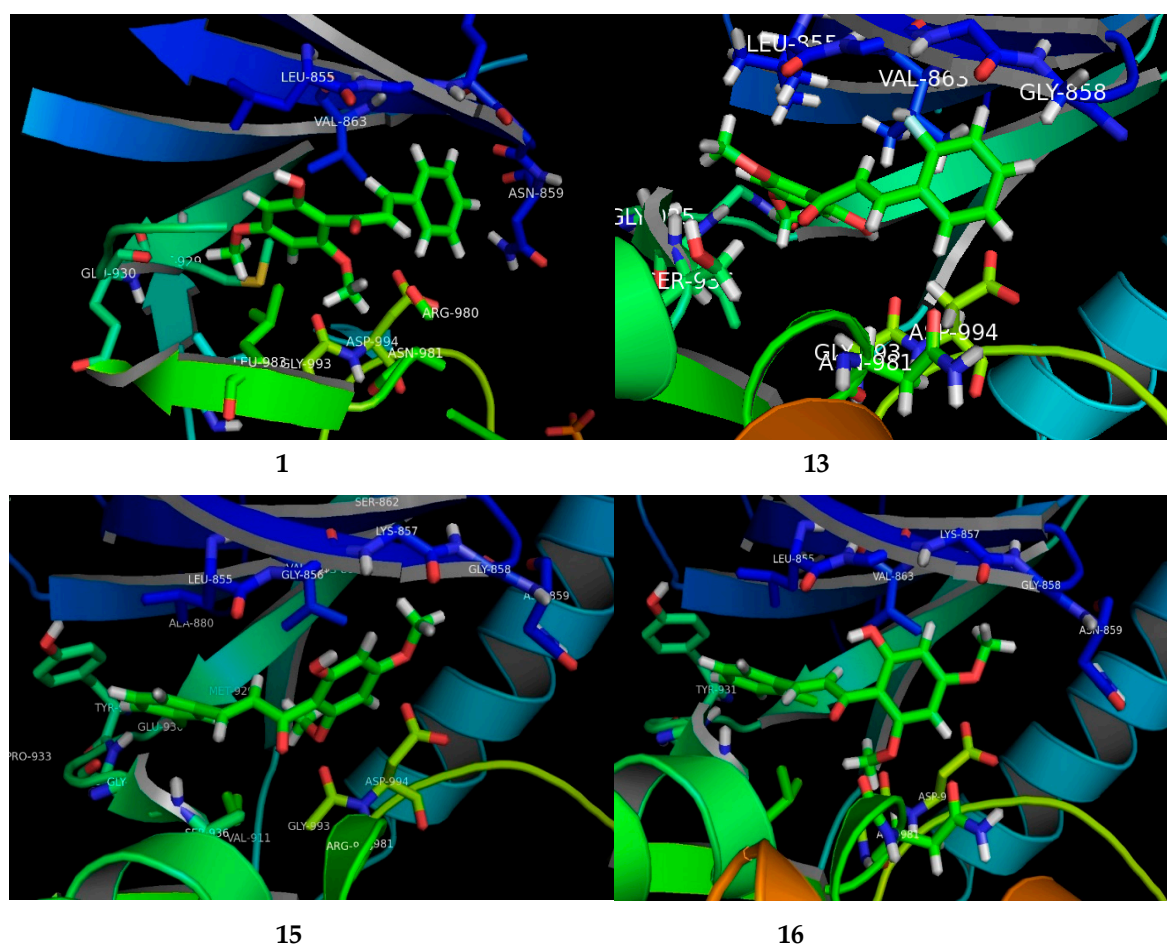
Figure 3. The visual presenting the interaction of FKB derivatives (**1**, **13**, **15** and **16**) with the ATP binding site of human JAK2 tyrosine kinase.

3. Materials and Methods

3.1. Chemistry

Melting points were determined on a Fisher–Johns melting apparatus and are uncorrected. UV spectra were recorded on UV-VIS spectrophotometer model of type Genesys 10s and expressed in nm. FT-IR spectroscopic studies were carried out on a FTIR spectrophotometer 1000, model Perkin

Elmer, at a room temperature of 25 °C. KBr pellets were dried in an oven and scanned for calibration purposes. ^{1}H-NMR spectra of compounds were recorded on a Bruker Ascend TM 600 MHz machine. The chemical shifts (δ) are presented with reference to CDCl$_3$ (δ: 7.25) and tetramethylsilane (TMS) (δ: 0.00) as the internal reference. Electron-spray ionization mass spectra in positive mode (ESI-MS) data were recorded on a Bruker Esquire 3000+ spectrometer. Column chromatography purifications were carried out on a Silica Gel 60 (Merck, 70–230 mesh). The purity of compounds was checked by thin-layer chromatography (TLC) and ^{1}H-NMR. All the chemicals were purchased from Sigma-Aldrich (Saint Louis, MO, USA). Other reagents were purchased from Sinopharm Chemical Reagent Co. Ltd., (Shanghai, China).

3.2. Docking Analysis Method

To rationalize the anti-cancer potential of FKB derivatives, the online web Prediction of Activity Spectra for Substances (PASS) server was used to predict the biological activity of potential FKB derivatives [49,50]. The information on the compounds was uploaded with the value of probability of activity (Pa) set to 0.7. The results were then analyzed critically to understand the molecular basis for the anti-cancer activity of the compounds. Molecular docking simulation of selected inhibitors against JAK2 was carried out using MOE [51]. The crystal structure of JAK2 in complex with a potent quinoxaline inhibitor, PDB:3KRR [52], was downloaded in MOE. The derivatives with potential IC$_{50}$ values (Table 2.) for compound **1**, **13**, **15** and **16** were subjected to rigid receptor docking, and the resulting poses were analyzed visually. All the graphics were rendered using MOE and Chimera [53]. To study the dynamic behavior of the proposed ligand–protein complex, we have performed in a short production run of 10 ns using AMBER 14 [54]. The resulting trajectories were analyzed using the CPPTRAJ module in AMBERTOOLS 16 [55,56].

3.3. Synthesis of Flavokawain B derivatives

KOH (20% *w*/*v* aqueous solution) was added to a stirred solution of the appropriate acetophenone (1.0 eq) and a substituted benzaldehyde (1.25 eq.) in ethanol, and the mixture was stirred at room temperature for 48–72 h. The reaction mixture was cooled to 0 °C (ice-water bath) and acidified with HCl (10% *v*/*v* aqueous solution). In most cases, yellow precipitate was formed, filtered and washed with 10% aqueous HCl solution. In the cases where an orange-yellow layer was formed, the mixture was extracted with CH$_2$Cl$_2$ or ethyl acetate, the extracts was dried over Na$_2$SO$_4$ anhydrous and the solvent was evaporated and crystalized with methanol or ethanol.

3.4. Characterization Data

The data of flavokawain B (**1**) and flavokawain A (**2**) have been published previously by us [26,57].

(E)-1-(2′-Hydroxy-4′,6′-dimethoxyphenyl)-3-(4-(methylthio)phenyl)prop-2-en-1-one (**3**). Orange crystal (78.3% yield); m.p.: 129–131 °C; UV-Vis (CHCl$_3$) λ_{max}: 371–372 nm; IR (KBr, cm^{-1}): 3469 (O-H), 2981–3014 (Ar C-H stretch), 1619 (C=O), 1548–1584 (C=C-C=O), 1431–1432 (Ar C=C), 1155–1218 (C-O) [36].

(E)-3-(2,3-Dimethoxyphenyl)-1-(2′-hydroxy-4′,6′-dimethoxyphenyl)prop-2-en-1-one (**4**). Yellow crystal (83.4% yield); m.p.: 121–123 °C (lit. [58] 120–122 °C); UV-Vis (MeOH)$_{\lambda max}$: 335–337 nm; IR (KBr, cm^{-1}): 3458 (O-H), 2839–2985 (Ar C-H stretch), 1627 (C=O), 1556–1581 (C=C-C=O), 1350–1442 (C=C), 1213–1268 (C-O); ^{1}H-NMR (600 MHz, CDCl$_3$) δ: 14.34 (s, 1H, OH, C-2′), 8.08 (d, 1H, H-β, *J* = 15.78 Hz), 7.96 (d, 1H, H-α, *J* = 15.78 Hz), 7.24 (d, 1H, H-6, *J* = 7.74 Hz), 7.08 (t, 1H, H-5, *J* = 8.04, 7.98 Hz), 6.95 (d, 1H, H-4, *J* = 8.04 Hz), 6.11 (d, 1H, H-3′, *J* = 2.10 Hz), 5.96 (d, 1H, H-5′, *J* = 2.10 Hz), 3.91 (s, 3H, OCH$_3$, C-6′), 3.90 (s, 3H, OCH$_3$, C-2), 3.89 (s, 3H, OCH$_3$, C-3), 3.84 (s, 3H, OCH$_3$, C-4′); ^{13}C-NMR (150 MHz, CDCl$_3$) δ: 192.93 (C=O), 168.40 (C-2), 166.18 (C-6′), 162.55 (C-4′), 153.24 (C-3), 148.88 (C-1), 137.19 (C-2′), 129.79 (C-5), 128.95 (C-6), 124.12 (C-4), 119.80 (C-5′), 113.76 (C-3′),

106.47 (C-1′), 93.70 (C-β), 91.20 (C-α), 61.31 (OCH$_3$), 55.92 (OCH$_3$), 55.84 (OCH$_3$), 55.58 (OCH$_3$); EI-MS: *m/z* = 344 (60), 329 (7), 313 (100), 207 (30), 181 (24), 180 (87), 164 (70), 152 (37), 149 (55), 137 (51), 121 (52), 91 (25), 77 (21), 69 (13); (Molecular formula C$_{19}$H$_{20}$O$_6$).

(E)-1-(2′-Hydroxy-4′,6′-dimethoxyphenyl)-3-(2,4,6-trimethoxyphenyl)prop-2-en-1-one (**6**). Orange crystal (82.8% yield); m.p.: 158–159 °C (lit. [59] 151–153 °C); UV-Vis (MeOH): λ$_{max}$: 386 nm; IR (KBr, cm^{-1}): 3464 (O-H), 2941–3010 (Ar C-H stretch), 1618 (C=O), 1414–1545 (C=C), 1122–1217 (C-O); ^{1}H-NMR (600 MHz, CDCl$_3$) δ; 14.76 (s, 1H, OH, C-2′), 8.32 (d, 1H, H-β, *J* = 15.78 Hz), 8.25 (d, 1H, H-α, *J* = 15.78 Hz), 6.13 (s, 2H, H-3 and H-5), 6.09 (d, 1H, H-3′, *J* = 2.40 Hz), 5.94 (d, 1H, H-5′, *J* = 2.40 Hz), 3.90 (s, 3H, OCH$_3$, C-6 and C-6′), 3.89 (s, 3H, OCH$_3$, C-2), 3.85 (s, 3H, OCH$_3$, C-4′), 3.82 (s, 3H, OCH$_3$, C-4); EI-MS: *m/z* = 374 (2), 344 (44), 329 (8), 313 (100), 281 (10), 207 (50), 181 (25), 180 (54), 164 (44), 152 (21), 149 (37), 137 (37), 121 (33), 105 (12), 91 (26), 77 (23), 69 (15); (Molecular formula C$_{20}$H$_{22}$O$_7$).

(E)-3-(2,5-Dimethoxyphenyl)-1-(2′-hydroxy-4′,6′-dimethoxyphenyl)prop-2-en-1-one (**8**). EI-MS: *m/z* = 344 (78), 327 (33), 282 (10), 207 (68), 191 (44), 181 (27), 164 (62), 152 (14), 151 (100), 137 (19); (Molecular formula C$_{19}$H$_{20}$O$_6$).

(E)-3-(2-Fluorophenyl)-1-(2′-hydroxy-4′,6′-dimethoxyphenyl)prop-2-en-1-one (**13**). EI-MS: *m/z* = 302 (100), 301 (100), 285 (19), 282 (45), 207 (100), 181 (100), 166 (28), 152 (24), 149 (28), 137 (67), 121 (44), 101 (88), 95 (51), 69 (52); (Molecular formula C$_{17}$H$_{15}$FO$_4$).

(E)-3-(4-Fluorophenyl)-1-(2′-hydroxy-4′,6′-dimethoxyphenyl)prop-2-en-1-one (**14**). Yellow flat crystal (80.7% yield); m.p.: 144–145 °C (lit. [17] 140–141 °C); UV-Vis (MeOH) λ$_{max}$: 342–343 nm; IR (KBr, cm^{-1}): 3460 (O-H), 2854–3118 (Ar C-H stretch), 1632 (C=O), 1573–1592 (C=C-C=O), 1345–1507 (C=C), 1115–1216 (C-O); ^{1}H-NMR (600 MHz, CDCl$_3$) δ: 14.28 (s, 1H, OH, C-2′), 7.82 (d, 1H, H-β, *J* = 15.60 Hz), 7.74 (d, 1H, H-α, *J* = 15.60 Hz), 7.59 (m, 1H, H-2), 7.58 (m, 1H, H-6), 7.10 (m, 1H, H-3), 7.09 (m, 1H, H-5), 6.11 (d, 1H, H-3′, *J* = 2.40 Hz), 5.96 (d, 1H, H-5′, *J* = 2.40 Hz), 3.92 (s, 3H, OCH$_3$, C-6′), 3.84 (s, 3H, OCH$_3$, C-4′); GC-MS: *m/z* = 302 (84), 301 (100), 285 (12), 274 (14), 207 (99), 181 (41), 153 (12), 137 (23), 121 (13), 101 (17), 69 (11); (Molecular formula C$_{17}$H$_{15}$FO$_4$).

(E)-3-(3-Chlorophenyl)-1-(2′-hydroxy-4′,6′-dimethoxyphenyl)prop-2-en-1-one (**15**). Yellow solid (83.1% yield); m.p.: 105–107 °C (lit. [60] 104–106 °C); UV-Vis (MeOH) λ$_{max}$: 338–339 nm; IR (KBr, cm^{-1}): 3460 (O-H), 2945–3014 (Ar C-H stretch), 1634 (C=O), 1567–1585 (C=C-C=O), 1342–1443 (C=C), 1213–1215 (C-O); ^{1}H-NMR (600 MHz, CDCl$_3$) δ: 14.19 (s, 1H, OH, C-2′), 7.86 (d, 1H, H-β, *J* = 15.60 Hz), 7.68 (d, 1H, H-α, *J* = 15.60 Hz), 7.57 (brs, 1H, H-2), 7.46 (m, 1H, H-5) 7.35 (m, 2H, H-4 and H-6), 6.11 (d, 1H, H-3′, *J* = 2.34 Hz), 5.97 (d, 1H, H-5′, *J* = 2.34 Hz), 3.93 (s, 3H, OCH$_3$, C-6′), 3.85 (s, 3H, OCH$_3$, C-4′); ^{13}C-NMR (150 MHz, CDCl$_3$) δ: 192.26 (C=O), 168.47 (C-2′), 166.46 (C-4′), 162.50 (C-6′), 140.45 (C-β), 137.45 (C-1), 134.83 (C-3), 130.12 (C-2), 129.84 (C-4), 128.86 (C-5), 127.88 (C-6), 126.62 (C-α), 106.26 (C-1′), 93.81 (C-3′), 91.33 (C-5′), 55.95 (OCH$_3$), 55.65 (OCH$_3$); EI-MS: *m/z* = 317 (1), 314 (90), 297 (10), 283 (68), 267 (7), 207 (100), 181 (65), 167 (16), 152 (19), 137 (27), 121 (22); (Molecular formula C$_{17}$H$_{15}$ClO$_4$).

(E)-3-(2-Chlorophenyl)-1-(2′-hydroxy-4′,6′-dimethoxyphenyl)prop-2-en-1-one (**16**). Yellow crystal (80.7% yield); m.p.: 132–134 °C (lit. [18] 135–136 °C); UV-Vis (MeOH) λ$_{max}$: 341–342 nm; IR (KBr, cm^{-1}): 3448 (O-H), 2957–3132 (Ar C-H stetch), 1632 (C=O), 1556–1585 (C=C-C=O), 1338–1435 (C=C), 1110–1219 (C-O), 745–748 (C-Cl); ^{1}H-NMR (600 MHz, CDCl$_3$) δ: 14.24 (s, 1H, OH, C-2′), 8.12 (d, 1H, H-β, *J* = 15.60 Hz), 7.85 (d, 1H, H-α, *J* = 15.60 Hz), 7.67 (m, 1H, H-6), 7.40 (m, 1H, H-3), 7.28 (m, 2H, H-4 and H-5), 6.08 (d, 1H, H-3′, *J* = 2.34 Hz), 5.93 (d, 1H, H-5′, *J* = 2.40 Hz), 3.88 (s, 3H, OCH$_3$, C-6′), 3.81 (s, 3H, OCH$_3$, C-4′); EI-MS: *m/z* = 318 (30), 301 (4), 283 (70), 267 (7), 207 (100), 181 (32), 165 (6), 152 (6), 137 (12), 101 (12), 69 (7); (Molecular formula C$_{17}$H$_{15}$ClO$_4$).

(E)-3-(4-Chlorophenyl)-1-(2′-hydroxy-4′,6′-dimethoxyphenyl)prop-2-en-1-one (**17**). Yellow crystal (84.3% yield); m.p.: 171–173 °C (lit. [61] 173–175 °C); UV-Vis (MeOH) λ_{max}: 342–343 nm; IR (KBr, cm^{-1}): 3420 (O-H), 2981–3018 (Ar C-H stretch), 1630 (C=O), 1488–1591 (C=C), 1217–1219 (C-O), 820–822 (C-Cl); ^{1}H-NMR (600 MHz, CDCl$_3$) δ: 14.24 (s, 1H, OH, C-2′), 7.85 (d, 1H, H-β, J = 15.60 Hz), 7.72 (d, 1H, H-α, J = 15.60 Hz), 7.53 (d, 1H, H-2, J = 8.46 Hz), 7.52 (d, 1H, H-6, J = 8.46 Hz), 7.38 (d, 1H, H-3, J = 8.46 Hz), 7.37 (d, 1H, H-5, J = 8.46 Hz), 6.11 (d, 1H, H-3′, J = 2.40 Hz), 5.96 (d, 1H, H-5′, J = 2.40 Hz), 3.92 (s, 3H, OCH$_3$, C-6′), 3.84 (s, 3H, OCH$_3$, C-4′); EI-MS: m/z = 318 (57), 301 (7), 283 (2), 207 (100), 181 (34), 165 (13), 152 (19), 137 (25), 111 (6), 102 (20); (Molecular formula C$_{17}$H$_{15}$ClO$_4$).

(E)-3-(4-Bromophenyl)-1-(2′-hydroxy-4′,6′-dimethoxyphenyl)prop-2-en-1-one (**18**). Yellow flat crystal (80.5% yield); m.p.: 165.8–167.5 °C (lit. [17] 150–151 °C); UV-Vis (MeOH) λ_{max}: 346 nm; IR (KBr, cm^{-1}): 3447 (O-H), 2949–3010 (Ar C-H stretch), 1633 (C=O), 1568–1590 (C=C-C=O), 1338–1488 (C=C), 1215–1218 (C-O); ^{1}H-NMR (500 MHz, CDCl$_3$) δ: 7.85 (d, 1H, H-β, J = 15.50 Hz), 7.68 (d, 1H, H-α, J = 15.50 Hz), 7.53 (d, 1H, H-2, J = 8.50 Hz), 7.51 (d, 1H, H-6, J = 8.50 Hz), 7.45 (d, 1H, H-3, J = 8.50 Hz), 7.43 (d, 1H, H-5, J = 8.50 Hz), 6.09 (d, 1H, H-3′, J = 2.00 Hz), 5.95 (d, 1H, H-5′, J = 2.50 Hz), 3.90 (s, 3H, OCH$_3$, C-6′), 3.83 (s, 3H, OCH$_3$, C-4′); ^{13}C-NMR (150 MHz, CDCl$_3$) δ: 192.31 (C=O), 168.45 (C-2′), 166.40 (C-4′), 162.48 (C-6′), 140.78 (C-β), 134.53 (C-1), 132.10 (C-3), 132.10 (C-5), 129.68 (C-2), 129.68 (C-6), 128.15 (C-α), 124.19 (C-4), 106.29 (C-1′), 93.85 (C-3′), 91.32 (C-5′), 55.89 (OCH$_3$), 55.61 (OCH$_3$); EI-MS: m/z = 363 (48), 362 (48), 346 (5), 281 (5), 209 (16), 207 [100], 181 (25), 152 (9); (Molecular formula C$_{17}$H$_{15}$BrO$_4$).

(E)-1-(2′-Hydroxy-4′,6′-dimethoxyphenyl)-3-(3-nitrophenyl)prop-2-en-1-one (**20**). Yellow cotton (82.6% yield); m.p.: 169–171 °C (lit. [61] 169–170 °C); UV-Vis (MeOH) λ_{max}: 336 nm; IR (KBr, cm^{-1}): 3460 (O-H), 2851–3092 (Ar C-H stretch), 1638 (C=O), 1583 (C=C-C=O), 1427–1525 (C=C), 1223–1225 (C-O); ^{1}H-NMR (500 MHz, CDCl$_3$) δ: 8.56 (brs, 1H, H-2), 8.30 (d, 1H, H-4, J = 8.20 Hz), 8.22 (d, 1H, H-6, J = 7.75 Hz), 8.15 (d, 1H, H-β, J = 15.70 Hz), 7.84 (d, 1H, H-α, J = 15.70 Hz), 7.78 (t, 1H, H-5, J = 7.95, 8.00 Hz), 6.17 (d, 1H, H-3′, J = 2.35 Hz), 6.14 (d, 1H, H-5′, J = 2.35 Hz), 4.04 (s, 3H, OCH$_3$, C-6′), 3.91 (s, 3H, OCH$_3$, C-4′); EI-MS: m/z = 329 (33), 301 (5), 281 (6), 254 (5), 207 (100), 181 (25), 152 (5), 95 (5), 73 (8); (Molecular formula C$_{17}$H$_{15}$NO$_6$).

(E)-3-(5-Bromo-2-hydroxyphenyl)-1-(2′-hydroxy-4′,6′-dimethoxyphenyl)prop-2-en-1-one (**22**). Yellow crystal (76.2% yield); m.p.: 166–168 °C (lit. [61] 177–178 °C); UV-Vis (MeOH) λ_{max}: 359 nm; IR (KBr, cm^{-1}): 3435 (O-H), 2945–2994 (Ar C-H stretch), 1623 (C=O), 1419–1590 (C=C), 1220–1221 (C-O); ^{1}H-NMR (600 MHz, CDCl$_3$) δ: 14.19 (s, 1H, OH, C-2′), 8.12 (d, 1H, H-β, J = 15.70 Hz), 8.01 (d, 1H, H-α, J = 15.70 Hz), 7.78 (brs, 1H, H-6), 7.39 (d, 1H, H-4, J = 8.70 Hz), 6.97 (d, 1H, H-3, J = 8.64 Hz), 6.13 (brs, 1H, H-3′), 6.12 (brs, 1H, H-5′), 3.98 (s, 3H, OCH$_3$, C-6′), 3.88 (s, 3H, OCH$_3$, C-4′); EI-MS: m/z = 379 (1), 364 (14), 333 (5), 305 (3), 281 (9), 251 (3), 227 (9), 214 (17), 207 (60), 191 (10), 142 (13), 115 (8), 95 (10), 73 (14); (Molecular formula C$_{17}$H$_{15}$BrO$_5$).

(E)-3-(2-Bromo-3-hydroxy-4-methoxyphenyl)-1-(2′-hydroxy-4′,6′-dimethoxyphenyl)prop-2-en-1-one (**23**). Orange crystal (85.6% yield); m.p.: 201–203 °C; UV-Vis (MeOH) λ_{max}: 366–369 nm; IR (KBr, cm^{-1}): 3425 (O-H), 2838–3014 (Ar C-H stretch), 1634 (C=O), 1496–1596 (C=C), 1213–1259 (C-O); EI-MS: m/z = 409 (4), 408 (4), 403 (3), 229 (3), 207 (3), 202 (3), 181 (2), 165 (3), 141 (4), 112 (5), 87 (4), 59 (4); (Molecular formula C$_{18}$H$_{17}$BrO$_6$).

3.5. X-ray Crystallographic Analysis

X-ray analysis for all these samples was performed using Bruker APEX II DUO CCD diffractometer, employing MoKα radiation (λ = 0.71073 Å) with φ and ω scans, at room temperature. Data reduction and absorption correction were performed using the SAINT and SADABS programs [62]. All structures were solved by direct methods and refined by full-matrix, least-squares techniques on F^2 using the SHELXTL software package [63]. Crystallographic data for the reported

structures have been deposited at the Cambridge Crystallographic Data Centre (CCDC) with the CCDC deposition numbers of 1548733 and 1548734. Copies of available material can be obtained free of charge on application to the CCDC, 12 Union Road, Cambridge CB2 1EZ, UK, (Fax: +44-(0)1223–336033 or e-mail: deposit@ccdc.cam.ac.uk). The ORTEP (Oak Ride Thermal Ellipsoid Plot Program) of compound **7** and **9** are shown in Figure 2 and X-ray crystallographic data presented in Table 3.

Table 3. Crystal data and parameters for the structure refinement of **7** and **9**.

Compound	7	9
CCDC Number	1548734	1548733
Molecular Formula	$C_{19}H_{20}O_6$	$C_{18}H_{18}O_5$
Molecular Weight	344.35	314.32
Crystal System	Triclinic	Orthorhombic
Space Group	$P\bar{1}$	*Pbca*
a (Å)	8.4560 (17)	14.447 (3)
b (Å)	8.4790 (17)	7.9755 (15)
c (Å)	12.549 (3)	26.203 (5)
α (°)	104.166 (3)	90
β (°)	92.063 (3)	90
γ (°)	106.227 (3)	90
V (Å^3)	832.4 (3)	3019.0 (10)
Z	2	8
Dcalc (g cm^{-3})	1.374	1.383
Crystal dimensions (mm)	$0.58 \times 0.18 \times 0.11$	$0.55 \times 0.27 \times 0.14$
μ (mm^{-1})	0.10	0.10
T_{min}/T_{max}	0.7665, 0.9584	0.8489, 0.9495
Reflections measured	28,367	14,974
Ranges/indices (h, k, l)	$-11{\rightarrow}11$; $-11{\rightarrow}11$; $-17{\rightarrow}17$	$-16{\rightarrow}16$; $-9{\rightarrow}9$; $-30{\rightarrow}28$
θ limit (°)	1.7$-$29.2	1.6$-$24.6
Unique reflections	4491	2516
Observed reflections ($I > 2\sigma(I)$)	2352	1594
Parameters	234	211
Goodness of fit on F^2	1.02	1.05
R_1, wR_2 [$I \geq 2\sigma(I)$]	0.055, 0.176	0.056, 0.156

3.6. Anticancer Activity

3.6.1. Sample preparation

Stock samples at 1 mg/mL of dimethyl sulfoxide (DMSO) (Sigma-Aldrich) were prepared and kept at 4 °C.

3.6.2. MTT Cell Viability Assay

Breast cancer MCF-7 and MDA-MB-231 cells were purchased from the American Type Culture Collection (ATCC, Manassas, VA, USA) and cultured at 37 °C, 5% CO_2 and 90% humidity using RPMI-1640 medium (Sigma-Aldrich) supplemented with 10% fetal bovine serum (FBS) (Thermo Fisher Scientific, USA). The MTT [3-(4,5-dimethylthiazol-2-yl)-2,5-diphenyltetrazolium bromide] method cell viability assay was conducted according to our previous report [64]. In brief, MCF-7 and MDA-MB-231 were seeded overnight in 96-well plates at 8×10^4 cells/well. All compounds were dissolved in dimethyl sulfoxide (DMSO, Sigma, St. Louis, MO, USA) to get a stock solution of 1 mg/mL and stored at 4 °C. Then, the compounds were serially diluted into the seeded cells at concentrations ranging between 30–0.47 μg/mL. Cells treated with 3% DMSO (Sigma) were used as a negative control. After 72 h of incubation, 20 μL of MTT solution (5 mg/mL) was added into all the wells and the plates were further incubated for another 3 hrs. Then, 170 μL of solution from all the wells were discarded and 100 μL of DMSO (Sigma) were added to dissolve the purple crystals. The absorbance was then recorded using an ELISA plate reader (Biotek Instruments, Winooski, VT, USA) at the wavelength of 570 nm. All samples were tested for triplicates. The percentage of cell viability was calculated using following formula:

$$\text{Cell viability (\%) = [OD sample at 570 nm/OD negative control at 570 nm]} \times 100\% \qquad (1)$$

The IC$_{50}$ value (concentration of compounds inhibited 50% of cell viability) was determined from the graph of cell viability vs absorbance.

4. Conclusions

Twenty-three FKB derivatives were synthesized by Claisen–Schmidt condensation reaction. Three FKB derivatives, namely **8**, **13** and **23**, were found to be new chalcones. The chalcones with electron-withdrawing and electron-donating substituents had effects on cytotoxicity. The FKB derivatives with electron-withdrawing groups in ring B, as in **13** (2F), **15** (3Cl) and **16** (2Cl), exhibited potential cytotoxic effects on breast cancer cell lines, while the presence of the substituted electron-donating groups, as in **4**, **5**, **9** and **10**, showed lower cytotoxic effects on MCF-7 and MDA-MB-231 cell lines. The FKB derivatives **16** (IC$_{50}$ = 6.50 ± 0.40 and 4.12 ± 0.20 μg/mL), **15** (IC$_{50}$ = 5.52 ± 0.35 and 6.50 ± 1.40 μg/mL) and **13** (IC$_{50}$ = 7.12 ± 0.80 and 4.04 ± 0.30 μg/mL) were found to be the most active compounds among the FKB series chalcones. The structure–activity relationship showed FKB chalcones with different substituents and effects on cytotoxicity. The FKB skeleton is unique for anticancer agents, additionally, the presence of halogens (Cl and F) in position two and three also improve the cytotoxicity of FKB (**1**). These findings could help to improve or find new drugs for future anti-cancer agents.

Author Contributions: Addila Abu Bakar, Muhammad Nadeem Akhtar and Seema Zareen carried out the literature, design and synthesis of chalcones (synthesis and purification), Swee Keong Yeap, Norlaily Mohd Ali and Noorjahan Banu Alitheen contributed to the study of cancer cell lines, Ching Kheng Quah and Wan-Sin Loh contributed to the X-ray analysis of the compounds. Zaheer Ul-Haq and Syed Adnan Ali Shah contributed to the docking analysis. All the authors read and approved the final manuscript.

Conflicts of Interest: The authors declare no conflict of interest.

References

1. Polyak, K. Breast cancer: Origins and evolution. *J. Clin. Investig.* **2007**, *117*, 3155–3163. [CrossRef] [PubMed]
2. Perou, C.M.; Sørlie, T.; Eisen, M.B.; Van de Rijn, M.; Jeffrey, S.S.; Rees, C.A.; Pollack, J.R.; Ross, D.T.; Johnsen, H.; Akslen, L.A.; et al. Molecular portraits of human breast tumours. *Nature* **2000**, *406*, 747–752. [CrossRef] [PubMed]
3. Sørlie, T.; Perou, C.M.; Tibshirani, R.; Aas, T.; Geisler, S.; Johnsen, H.; Hastie, T.; Eisen, M.B.; Van de Rijn, M.; Jeffrey, S.S.; et al. Gene expression patterns of breast carcinomas distinguish tumor subclasses with clinical implications. *PNAS* **2001**, *98*, 10869–10874. [CrossRef] [PubMed]
4. Rao, S.D.; Kumar, P.G.; Harika, G.; Pooja, B.; Rao, S.; Kumar, A.Y. Recent advances and potential pharmacological activities of chalcones and their heterocyclic derivatives a valuable insight. *J. Chem. Pharm. Res.* **2016**, *8*, 458–477.
5. Patil, C.B.; Mahajan, S.K.; Katti, S.A. Chalcone: A Versatile Molecule. *J. Pharm. Sci. Res.* **2009**, *1*, 11–22.
6. Dyrager, C.; Wickström, M.; Fridén-Saxin, M.; Friberg, A.; Dahlén, K.; Wallén, E.A.A.; Gullbo, J.; Grøtli, M.; Luthman, K. Inhibitors and promoters of tubulin polymerization: Synthesis and biological evaluation of chalcones and related dienones as potential anticancer agents. *Bioorg. Med. Chem.* **2011**, *19*, 2659–2665. [CrossRef] [PubMed]
7. Echeverria, C.; Santibañez, J.F.; Donoso-Tauda, O.; Escobar, C.A.; Ramirez-Tagle, R. Structural Antitumoral Activity Relationships of Synthetic Chalcones. *Int. J. Mol. Sci.* **2009**, *10*, 221–231. [CrossRef] [PubMed]

8. Ilango, K.; Valentina, P.; Saluja, G.S. Synthesis and in vitro anticancer activity of some substituted chalcone derivatives. *Res. J. Pharm. Biol. Chem. Sci.* **2010**, *1*, 354–359.

9. Kamal, A.; Ramakrishna, G.; Raju, P.; Viswanath, A.; Ramaiah, M.J.; Balakishan, G.; Pal-Bhadra, M. Synthesis and anti-cancer activity of chalcone linked imidazolones. *Bioorg. Med. Chem. Lett.* **2010**, *20*, 4865–4869. [CrossRef] [PubMed]

10. Szliszka, E.; Czuba, Z.P.; Mazur, B.; Sedek, L.; Paradysz, A.; Krol, W. Chalcones Enhance TRAIL-Induced Apoptosis in Prostate Cancer Cells. *Int. J. Mol. Sci.* **2010**, *11*, 1–13. [CrossRef] [PubMed]

11. Bandgar, B.P.; Gawande, S.S.; Bodade, R.G.; Totre, J.V.; Khobragade, C.N. Synthesis and biological evaluation of simple methoxylated chalcones as anticancer, anti-inflammatory and antioxidant agents. *Bioorg. Med. Chem.* **2010**, *18*, 1364–1370. [CrossRef] [PubMed]

12. Herencia, F.; Lo, M.P.; Ubeda, A.; Ferrándiz, M.L. Nitric oxide-scavenging properties of some chalcone derivatives. *Nitric Oxide* **2002**, *6*, 242–246. [CrossRef] [PubMed]

13. Yadav, H.L.; Gupta, P.; Pawar, R.S.; Singour, P.K.; Patil, U.K. Synthesis and biological evaluation of anti-inflammatory activity of 1,3 diphenyl propenone derivatives. *Med. Chem. Res.* **2010**, *20*, 461–465. [CrossRef]

14. Zhang, X.W.; Zhao, D.H.; Quan, Y.C.; Sun, L.P.; Yin, X.M.; Guan, L.P. Synthesis and evaluation of antiinflammatory activity of substituted chalcone derivatives. *Med. Chem. Res.* **2010**, *19*, 403–412. [CrossRef]

15. Awasthi, S.K.; Mishra, N.; Kumar, B.; Sharma, M.; Bhattacharya, A.; Mishra, L.C.; Bhasin, V.K. Potent antimalarial activity of newly synthesized substituted chalcone analogs in vitro. *Med. Chem. Res.* **2009**, *18*, 407–420. [CrossRef]

16. Hans, R.H.; Guantai, E.M.; Lategan, C.; Smith, P.J.; Wan, B.; Franzblau, S.G.; Gut, J.; Rosenthal, P.J.; Chibale, K. Synthesis, antimalarial and antitubercular activity of acetylenic chalcones. *Bioorg. Med. Chem. Lett.* **2010**, *20*, 942–944. [CrossRef] [PubMed]

17. Boeck, P.; Falcão, C.A.B.; Leal, P.C.; Yunes, R.A.; Filho, V.C.; Torres-Santos, E.C.; Rossi-Bergmann, B. Synthesis of chalcone analogues with increased antileishmanial activity. *Bioorg. Med. Chem.* **2006**, *14*, 1538–1545. [CrossRef] [PubMed]

18. Roussaki, M.; Lima, S.C.; Kypreou, A.M.; Kefalas, P.; Silva, A.C.D.; Detsi, A. Aurones: A promising heterocyclic scaffold for the development of potent antileishmanial agents. *Int. J. Med. Chem.* **2012**, *2012*, 1–8. [CrossRef] [PubMed]

19. Zainuri, D.A.; Arshad, S.; Khalib, N.C.; Razak, I.A.; Pillai, R.R.; Sulaiman, S.F.; Hashim, N.S.; Ooi, K.L.; Armaković, S.; Armaković, S.J.; et al. Synthesis, XRD crystal structure, spectroscopic characterization (FT-IR, ^{1}H and ^{13}C NMR), DFT studies, chemical reactivity and bond dissociation energy studies using molecular dynamics simulations and evaluation of antimicrobial and antioxidant activities of a novel chalcone derivative, (*E*)-1-(4-bromophenyl)-3-(4-iodophenyl)prop-2-en-1-one. *J. Mol. Struct.* **2017**, *1128*, 520–533. [CrossRef]

20. Wang, Y.H.; Dong, H.H.; Zhao, F.; Wang, J.; Yan, F.; Jiang, Y.Y.; Jin, Y.S. The synthesis and synergistic antifungal effects of chalcones against drug resistant *Candida albicans*. *Bioorg. Med. Chem. Lett.* **2016**, *26*, 3098–3102. [CrossRef] [PubMed]

21. Doan, T.N.; Tran, D.T. Synthesis, Antioxidant and Antimicrobial Activities of a Novel Series of Chalcones, Pyrazolic Chalcones, and Allylic Chalcones. *Pharmacol. Pharm.* **2011**, *2*, 282–288. [CrossRef]

22. Shenvi, S.; Kumar, K.; Hatti, K.S.; Rijesh, K.; Diwakar, L.; Reddy, G.C. Synthesis, anticancer and antioxidant activities of 2,4,5-trimethoxy chalcones and analogues from asaronaldehyde: Structure-activity relationship. *Eur. J. Med. Chem.* **2013**, *62*, 435–442. [CrossRef] [PubMed]

23. Sivakumar, P.M.; Prabhakar, P.K.; Doble, M. Synthesis, antioxidant evaluation, and quantitative structure-activity relationship studies of chalcones. *Med. Chem. Res.* **2011**, *20*, 482–492. [CrossRef]

24. Kaushik, S.; Kumar, N.; Drabu, S. Synthesis and anticonvulsant activities of phenoxychalcones. *Pharma Res.* **2010**, *3*, 257–262.

25. Sukumaran, S.D.; Chee, C.F.; Viswanathan, G.; Buckle, M.J.; Othman, R.; Abd Rahman, N.; Chung, L.Y. Synthesis, Biological Evaluation and Molecular Modelling of 2′-Hydroxychalcones as Acetylcholinesterase Inhibitors. *Molecules* **2016**, *21*, 955. [CrossRef] [PubMed]

26. Akhtar, M.N.; Sakeh, N.M.; Zareen, S.; Gul, S.; Lo, K.M.; Ul-Haq, Z.; Shah, S.A.A.; Ahmad, S. Design and synthesis of chalcone derivatives as potent tyrosinase inhibitors and their structural activity relationship. *J. Mol. Struct.* **2015**, *1085*, 97–103. [CrossRef]

27. Chimenti, F.; Fioravanti, R.; Bolasco, A.; Chimenti, P.; Secci, D.; Rossi, F.; Yáñez, M.; Orallo, F.; Ortuso, F.; Alcaro, S. Chalcones: A valid scaffold for monoamine oxidases inhibitors. *J. Med. Chem.* **2009**, *52*, 2818–2824. [CrossRef] [PubMed]

28. Dharmaratne, H.R.W.; Nanayakkara, N.P.D.; Khan, I.A. Kavalactones from *Piper methysticum*, and their ¹³C-NMR spectroscopic analyses. *Phytochemistry* **2002**, *59*, 429–433. [CrossRef]

29. Abu, N.; Ho, W.Y.; Yeap, S.K.; Akhtar, M.N.; Abdullah, M.P.; Omar, A.R.; Alitheen, N.B. The flavokawain: Uprising medicinal chalcones. *Cancer Cell Int.* **2013**, *13*, 1–7. [CrossRef] [PubMed]

30. Abu, N.; Mohamed, N.E.; Yeap, S.K.; Lim, K.L.; Akhtar, M.N.; Zulfadli, A.J.; Kee, B.B.; Abdullah, M.P.; Omar, A.R.; Alitheen, N.B. In vivo antitumor and antimetastatic effects of flavokawain B in 4T1 breast cancer cell-challenged mice. *Drug Des. Dev. Ther.* **2015**, *9*, 1401–1417. [CrossRef]

31. Abu, N.; Akhtar, M.N.; Yeap, S.K.; Lim, K.L.; Ho, W.Y.; Abdullah, M.P.; Ho, C.L.; Omar, A.R.; Ismail, J.; Alitheen, N.B. Flavokawain B induced cytotoxicity in two breast cancer cell lines, MCF-7 and MDA-MB231 and inhibited the metastatic potential of MDA-MB231 via the regulation of several tyrosine kinases in vitro. *BMC Complement. Altern. Med.* **2016**, *16*, 1–14. [CrossRef] [PubMed]

32. Kamaldin, M.N.; Akhtar, M.N.; Mohamad, A.S.; Lajis, N.; Perimal, E.K.; Akira, A.; Ming-Tatt, L.; Israf, D.A.; Sulaiman, M.R. Peripheral antinociception of a chalcone, flavokawin B and possible involvement of the nitric oxide/cyclic guanosine monophosphate/potassium channels pathway. *Molecules* **2013**, *18*, 4209–4220. [CrossRef] [PubMed]

33. Mohamad, A.S.; Akhtar, M.N.; Khalivulla, S.I.; Perimal, E.K.; Khalid, M.H.; Ong, H.M.; Zareen, S.; Akira, A.; Israf, D.A.; Lajis, N.; et al. Possible Participation of Nitric Oxide/Cyclic Guanosine Monophosphate/Protein Kinase C/ATP-Sensitive K+ Channels Pathway in the Systemic Antinociception of Flavokawin B. *Basic Clin. Pharmacol. Toxicol.* **2011**, *108*, 400–405. [CrossRef] [PubMed]

34. Abu, N.; Akhtar, M.N.; Yeap, S.K.; Lim, K.L.; Ho, W.Y.; Zulfadli, A.J.; Omar, A.R.; Sulaiman, M.R.; Abdullah, M.P.; Alitheen, N.B. Flavokawain A induces apoptosis in MCF-7 and MDA-MB231 and inhibits the metastatic process in vitro. *PLoS ONE* **2014**, *9*, 1–12. [CrossRef] [PubMed]

35. Abu, N.; Mohamed, N.E.; Yeap, S.K.; Lim, K.L.; Akhtar, M.N.; Zulfadli, A.J.; Kee, B.B.; Abdullah, M.P.; Omar, A.R.; Alitheen, N.B. In Vivo Anti-Tumor Effects of Flavokawain A in 4T1 Breast Cancer Cell-Challenged Mice. *Anticancer Agents Med. Chem.* **2015**, *15*, 905–915. [CrossRef] [PubMed]

36. Ali, N.M.; Akhtar, M.N.; Ky, H.; Lim, K.L.; Abu, N.; Zareen, S.; Ho, W.Y.; Alan-Ong, H.K.; Tan, S.W.; Alitheen, N.B.; et al. Flavokawain derivative FLS induced G2/M arrest and apoptosis on breast cancer MCF-7 cell line. *Drug Des. Dev. Ther.* **2016**, *10*, 1897–1907. [CrossRef]

37. Bandgar, B.P.; Patil, S.A.; Gacche, R.N.; Korbad, B.L.; Hote, B.S.; Kinkar, S.N.; Jalde, S.S. Synthesis and biological evaluation of nitrogen-containing chalcones as possible anti-inflammatory and antioxidant agents. *Bioorg. Med. Chem. Lett.* **2010**, *20*, 730–733. [CrossRef] [PubMed]

38. Mai, C.W.; Yaeghoobi, M.; Abd-Rahman, N.; Kang, Y.B.; Pichika, M.R. Chalcones with electron-withdrawing and electron-donating substituents: Anticancer activity against TRAIL resistant cancer cells, structure-activity relationship analysis and regulation of apoptotic proteins. *Eur. J. Med. Chem.* **2014**, *77*, 378–387. [CrossRef] [PubMed]

39. Pouget, C.; Lauthier, F.; Simon, A.; Fagnere, C.; Basly, J.P.; Delage, C.; Chulia, A.J. Flavonoids: Structural Requirements for Antiproliferative Activity on Breast Cancer Cells. *Bioorg. Med. Chem. Lett.* **2001**, *11*, 3095–3097. [CrossRef]

40. Jin, F.; Jin, X.Y.; Jin, Y.L.; Sohn, D.W.; Kim, S.A.; Sohn, D.H.; Kim, Y.C.; Kim, H.S. Structural Requirements of 2′,4′,6′-Tris(methoxymethyl) chalcone Derivatives for Anti-inflammatory Activity: The Importance of a 2′-Hydroxy Moiety. *Arch. Pharm. Res.* **2007**, *30*, 1359–1367. [CrossRef] [PubMed]

41. Nakhjiri, M.; Safavi, M.; Alipour, E.; Emami, S.; Atash, A.F.; Jafari-Zavareh, M.; Ardestani, S.K.; Khoshneviszadeh, M.; Foroumadi, A.; Shafie, A. Asymmetrical 2,6-bis(benzylidene)cyclohexanones: Synthesis, cytotoxic activity and QSAR study. *Eur. J. Med. Chem.* **2012**, *50*, 113–123. [CrossRef] [PubMed]

42. Alnemri, E.S.; Livingston, D.J.; Nicholson, D.W.; Salvesen, G.; Thornberry, N.A.; Wong, W.W.; Yuan, J. Human ICE/CED-3 Protease Nomenclature. *Cell* **1996**, *87*, 171. [CrossRef]

43. Molecular Operating Environment (MOE). Available online: https://www.chemcomp.com/MOE-Molecular_Operating_Environment.htm (accessed on 23 November 2017).

44. Baffert, F.; Régnier, C.H.; De Pover, A.; Pissot-Soldermann, C.; Tavares, G.A.; Blasco, F.; Brueggen, J.; Chéne, P.; Drueckes, P.; Erdmann, D.; et al. Potent and selective inhibition of polycythemia by the quinoxaline JAK2 inhibitor NVP-BSK805. *Mol. Cancer Ther.* **2010**, *9*, 1945–1955. [CrossRef] [PubMed]

45. Pettersen, E.F.; Goddard, T.D.; Huang, C.C.; Couch, G.S.; Greenblatt, D.M.; Meng, E.C.; Ferrin, T.E. UCSF Chimera—A visualization system for exploratory research and analysis. *J. Comput. Chem.* **2004**, *25*, 1605–1612. [CrossRef] [PubMed]

46. Case, D.A.; Cheatham III, T.E.; Darden, T.; Gohlke, H.; Luo, R.; Merz, K.M., Jr.; Onufriev, A.; Simmerling, C.; Wang, B.; Woods, R.J. The Amber Biomolecular Simulation Programs. *J. Comput. Chem.* **2005**, *26*, 1668–1688. [CrossRef] [PubMed]

47. Roe, D.R.; Cheatham, T.E., III. PTRAJ and CPPTRAJ: Software for processing and analysis of molecular dynamics trajectory data. *J. Chem. Theory Comput.* **2013**, *9*, 3084–3095. [CrossRef] [PubMed]

48. Case, D.A.; Betz, R.M.; Cerutti, D.S.; Cheatham III, T.E.; Darden, T.A.; Duke, R.E.; Giese, T.J.; Gohlke, H.; Goetz, A.W.; Homeyer, N.; Izadi, S.; et al. *AMBER 2016 Reference Manual*; University of California: San Francisco, CA, USA, 2016; pp. 1–923.

49. Lagunin, A.; Stepanchikova, A.; Filimonov, D.; Poroikov, V. PASS: prediction of activity spectra for biologically active substances. *Bioinformatics* **2000**, *16*, 747–748. [CrossRef] [PubMed]

50. Kadir, F.A.; Kassim, N.M.; Abdulla, M.A.; Yehye, W.A. Hepatoprotective Role of Ethanolic Extract of Vitex negundo in Thioacetamide-Induced Liver Fibrosis in Male Rats. *Evid. Based Complement. Alternat. Med.* **2013**, *2013*, 1–9. [CrossRef] [PubMed]

51. Jänicke, R.U.; Sprengart, M.L.; Wati, M.R.; Porter, A.G. Caspase-3 Is Required for DNA Fragmentation and Morphological Changes Associated with Apoptosis. *J. Biol. Chem.* **1998**, *273*, 9357–9360. [CrossRef] [PubMed]

52. Yang, X.H.; Sladek, T.L.; Liu, X.; Butler, B.R.; Froelich, C.J.; Thor, A.D. Reconstitution of Caspase 3 Sensitizes MCF-7 Breast Cancer Cells to Doxorubicin- and Etoposide-induced Apoptosis. *Cancer Res.* **2001**, *61*, 348–354. [PubMed]

53. Fulda, S.; Debatin, K.M. Caspase activation in cancer therapy. In *Madame Curie Bioscience Database [Internet]*; Landes Bioscience: Austin, TX, USA, 2013; pp. 1–29.

54. Sun, H.; Nikolovska-Coleska, Z.; Lu, J.; Qiu, S.; Yang, C.Y.; Gao, W.; Meagher, J.; Stuckey, J.; Wang, S. Design, synthesis, and evaluation of a potent, cell-permeable, conformationally constrained second mitochondria derived activator of caspase (Smac) mimetic. *J. Med. Chem.* **2006**, *49*, 7916–7920. [CrossRef] [PubMed]

55. Cheung, C.S.F.; Chung, K.K.W.; Lui, J.C.K.; Lau, C.P.; Hon, P.M.; Chan, J.Y.W.; Fung, K.P.; Au, S.W.N. Leachianone A as a potential anti-cancer drug by induction of apoptosis in human hepatoma HepG2 cells. *Cancer Lett.* **2007**, *253*, 224–235. [CrossRef] [PubMed]

56. Kiss, R.; Sayeski, P.P.; Keserű, G.M. Recent developments on JAK2 inhibitors: A patent review. *Expert Opin. Ther. Pat.* **2010**, *20*, 471–495. [CrossRef] [PubMed]

57. Mohamad, A.S.; Akhtar, M.N.; Zakaria, Z.A.; Perimal, E.K.; Khalid, S.; Mohd, P.A.; Khalid, M.H.; Israf, D.A.; Lajis, N.H.; Sulaiman, M.R. Antinociceptive activity of a synthetic chalcone, flavokawain B on chemical and thermal models of nociception in mice. *Eur. J. Pharmacol.* **2010**, *647*, 103–109. [CrossRef] [PubMed]

58. Srinivas, K.V.N.S.; Koteswara Rao, Y.; Mahender, I.; Das, B.; Rama Krishna, K.V.S.; Hara Kishore, K.; Murty, U.S.N. Flavanoids from Caesalpinia pulcherrima. *Phytochemistry* **2003**, *63*, 789–793. [CrossRef]

59. Rao, Y.K.; Fang, S.H.; Tzeng, Y.M. Differential effects of synthesized 2′-oxygenated chalcone derivatives: modulation of human cell cycle phase distribution. *Bioorg. Med. Chem.* **2004**, *12*, 2679–2686. [CrossRef] [PubMed]

60. Chiaradia, L.D.; Mascarello, A.; Purificação, M.; Vernal, J.; Cordeiro, M.N.S.; Zenteno, M.E.; Villarino, A.; Nunes, R.J.; Yunes, R.A.; Terenzi, H. Synthetic chalcones as efficient inhibitors of *Mycobacterium tuberculosis* protein tyrosine phosphatase PtpA. *Bioorg. Med. Chem. Lett.* **2008**, *18*, 6227–6230. [CrossRef] [PubMed]

61. Srinivasarao, V.; Krishna, C.R.; Ramesh, M.; Parthasarathy, T. Synthesis, in vitro anticancer activity evaluation and docking investigations of novel aromatic chalcones. *Mod. Chem.* **2013**, *1*, 1–7. [CrossRef]

62. Bruker, S. *APEX2 and SAINT*; Bruker AXS Inc.: Madison, WI, USA, 2009.

63. Sheldrick, G.M. A short History of SHELX. *Acta Cryst. A* **2008**, *64*, 112–122. [CrossRef] [PubMed]

64. Mosmann, T. Rapid colorimetric assay for cellular growth and survival: Application to proliferation and cytotoxicity assays. *J. Immunol. Methods* **1983**, *65*, 55–63. [CrossRef]

Sample Availability: Samples of the compounds **1**–**23** are available from the authors.